Iron Is a Physiological Ligand of SecA-like Metal Binding Domains

Tamar Cranford Smith[a,1], Mohammed Jamshad[a,1], Mark Jeeves[b], Mashael Alanazi[a,c], Cailean Carter[a], Janet E. Lovett[d], Timothy Knowles[a] and Damon Huber[a,*]

[a]Institute for Microbiology and Infection, [b]Institute of Cancer and Genomic Sciences and [d]School of Chemistry, University of Birmingham, Birmingham, United Kingdom; [c]Department of Biology, College of Science, Jouf University, Saudi Arabia; [d]SUPA, School of Physics and Astronomy and BSRC, University of St Andrews, St. Andrews, United Kingdom

Running title: *SecA-like MBDs bind to iron*

[1]These authors contributed equally to this work.

*Address correspondence to: Damon Huber, d.huber@bham.ac.uk

Keywords: SecA, Sec, protein translocation, metal binding, iron, zinc, NMR, EPR

ABSTRACT

The ATPase SecA is required for translocation of most proteins across the cytoplasmic membrane in bacteria. In *Escherichia coli*, SecA contains a small metal binding domain (MBD) at its extreme C-terminus that is widely conserved in other bacterial species and is required for its interaction with SecB. The MBD is thought to coordinate Zn^{2+} *via* a conserved cysteine-containing motif. Here, we investigated the metal binding properties of two *E. coli* proteins that contain SecA-like MBDs: YecA and YchJ. Both proteins copurify with metal, predominantly zinc. However, both proteins also copurify with significant amounts of iron. In YecA, iron binding is mediated by the MBD. Re-evaluation of the metal-binding properties of SecA indicate that: (i) SecA copurifies with stoichiometric amounts of iron; (ii) binding is mediated by the MBD; (iii) the MBD binds to iron with equal or greater affinity than to zinc; and (iv) the affinity for iron (but not for zinc) is mediated by a highly conserved serine in the metal-binding motif. Taken together, our results suggest that iron is a physiological ligand of SecA-like MBDs.

INTRODUCTION

Translocation of proteins across the cytoplasmic membrane is carried out by the Sec machinery (1,2). The central component of this machinery is a channel in the cytoplasmic membrane, which is composed of the proteins SecY, -E and -G in bacteria (3). The translocation of a subset of proteins through SecYEG requires the activity of the ATPase SecA (4,5). The SecA proteins of many bacterial species contain a small metal binding domain (MBD) at its extreme C-terminus (6), and in species that contain an MBD, its sequence is highly conserved (**figure 1A**). The MBD binds to a single Zn^{2+} ion, which is coordinated by three conserved cysteines and a histidine with the motif $CXCX_8C(H/C)$ (**figure 1A**) (6,7). In *Escherichia coli*, the MBD mediates the interaction of SecA with SecB (7,8), a chaperone that assists in the translocation of a subset of SecA substrate proteins (9). In addition, the MBD contains several conserved residues that are not obviously involved in binding to Zn^{2+} or SecB (6,10).

In this work, we investigated the metal binding properties of two *E. coli* proteins that contain SecA-like MBDs: YecA and YchJ (**Figure 1A**) (11,12). YecA contains an N-terminal UPF0149 domain and a C-terminal MBD. YchJ contains N- and C-terminal MBDs, which flank a UPF0225 domain. We purified YecA and YchJ and identified the copurifying metals. Although both proteins copurified predominantly with zinc, mass spectrometry and absorbance spectroscopy indicated that a significant fraction of the proteins copurified with iron. NMR and EPR spectroscopy indicated that YecA binds to iron *via* the MBD. These results prompted us to re-examine the metal-binding properties of the MBD of SecA.

SecA copurified with iron in stoichiometric amounts, and a peptide consisting of the MBD displayed a binding preference for iron. These results indicate that iron is a physiological ligand of SecA-like MBDs.

RESULTS

Mass spectrometry analysis of metals that co-purify with YecA and YchJ. To investigate the metal-binding properties of the MBDs of YecA and YchJ, we purified fusion proteins between YecA or YchJ and hexahistidine-tagged SUMO from *Saccharomyces cerevisiae* and determined the amount of copurifying manganese, iron, cobalt, copper and zinc by ICP-MS (**figure 1B**). YecA co-purified with zinc at a stoichiometry of 0.84 ± 0.03, and YchJ co-purified with zinc at a stoichiometry of 1.30 ± 0.17. The amount of copurifying zinc was consistent with the number of MBDs in each protein. Both proteins also copurified with lower, but detectable, amounts of copper (0.17 ± 0.11 for YecA; 0.02 ± 0.01 for YchJ) and iron (0.04 ± 0.03 for YecA; 0.05 ± 0.04 for YchJ).

Absorbance spectroscopy of purified YecA and YchJ. During purification, the colour of the YecA- and YchJ-bound Ni-NTA columns was yellow. If TCEP was included in the buffers used for purification of YecA, the Ni-NTA column remained yellow after elution of the bound protein (**supporting figure S1A**), and the EDTA eluate contained a large amount of iron (**supporting figure S1B**). Purified YecA and YchJ were pale yellow in colour and gradually became colourless with incubation at 4°C—typically over a period of one to several hours. YecA absorbed light with a peak at ~330 nm, and YchJ absorbed light with a peak at ~340 nm (**figure 2A**). Dialysis of YecA against buffer containing EDTA resulted in a decrease in absorbance at 330 nm (**figure 2B**), and the addition of an equimolar concentration of $FeSO_4$ restored absorbance of YecA at 330 nm (**figure 2B**), suggesting that the yellow colour of the purified YecA protein was due to coordination of Fe^{2+} (or potentially Fe^{3+}). Dialysis of YchJ against EDTA resulted in aggregation. Consequently, we did not investigate YchJ further.

EPR analysis of Fe^{3+} binding by YecA. To confirm that YecA can bind iron, we investigated the interaction of YecA with Fe^{3+} using EPR spectroscopy. (Fe^{2+} is not detectable by EPR.) The addition of a stoichiometric amount of purified metal-free YecA to a solution of Fe^{3+} (**figure 2C, blue line**) resulted in a new feature at 0.6145 T that is ~g = 4 (**figure 2C, red line**), indicating that there was a change in the electronic environment of the iron and indicating that YecA can bind to Fe^{3+}.

Identification of the iron-coordinating domain in YecA by NMR spectroscopy. To determine which domain was responsible for binding to iron, we purified ^{15}N- and ^{13}C-labelled YecA and investigated its structure using NMR spectroscopy. We could assign the resonances for the C-terminal 20 amino acids in the TROSY spectrum of the protein (excluding Pro-206 and Pro-208, which do not contain an N-H bond) (**figure 3A**). Several amino acids, including Arg-203, Asp-204, Asp-205, Leu-220 and His-221, produced two resonances, suggesting that the MBD in the metal-free protein exists in two distinct conformations (**figure 3A**). Addition of $FeSO_4$ resulted in the broadening and flattening of most of the resonances from amino acids in the MBD due to the paramagnetic properties of iron, but it affected very few of the resonances from the N-terminal ~200 amino acids (**figure 3B**). This result suggested that the MBD of YecA binds iron.

Co-purification of SecA-biotin with iron. The similarity of the MBDs of YecA and YchJ to the MBD of SecA suggested that SecA might also bind iron (**figure 1A**). Purification of SecA normally involves overproduction of the protein, which could lead to competition between metal ligands *in vivo*, followed by multiple purification steps, which could lead to metal exchange *in vitro*. To avoid these issues, we produced SecA from a chromosomally encoded, IPTG-inducible copy of the *secA* gene. The SecA produced by these strains contained a C-terminal tag that caused it to be biotinylated (SecA-biotin) (13) and allowed us to purify it using streptavidin-coated sepharose beads. SDS-PAGE indicated that the purified protein samples contained only two proteins: SecA and unconjugated streptavidin (**supporting figure S2**). ICP-OES indicated that SecA copurified with stoichiometric amounts of iron and lower amounts of zinc (**figure 4A**), suggesting that SecA binds preferentially to iron *in vivo*.

EPR analysis of Fe^{3+} binding by the SecA MBD. To demonstrate that the SecA MBD can bind to iron, we investigated the effect of the

MBD on the EPR spectrum of Fe^{3+}. The addition of a metal-free synthetic peptide consisting of the C-terminal 27 amino acids of SecA (SecA-MBD) caused a large increase in the EPR signal of Fe^{3+} at 1.2155 T (~g = 2) and altered the shape of the EPR spectrum (**figure 4B**). SecA-MBD also inhibited the formation of iron oxides in solutions containing $FeSO_4$ (**supporting figure S3**). These results indicated that SecA-MBD can bind iron.

^{1}H-NMR analysis of metal binding by SecA-MBD. We investigated binding of the SecA-MBD peptide to zinc and iron using ^{1}H-NMR. Consistent with previous studies (6), the addition of $ZnSO_4$ to SecA-MBD resulted in multiple changes in its ^{1}H-NMR spectrum including the appearance of resonances in the 8.5-9.5 ppm region, indicative of the formation of secondary structure (**figure 5A, blue and green traces**). The addition of $FeSO_4$ resulted in a broadening and flattening of most of the ^{1}H resonances (**figure 5A, red trace**). This effect was due to binding to iron since $FeSO_4$ did not affect the spectra of control peptides that do not bind iron.

We next investigated the ability of zinc to compete with iron for binding to SecA-MBD. To this end, we monitored the resonances of ^{1}H signals from the valine methyl groups, which displayed differences distinctive of its metal-bound state (**figure 5B**). The dissociation rate of Zn^{2+} from the MBD is relatively rapid (half-life of minutes) (7). However, the addition of $ZnSO_4$ to SecA-MBD that had been pre-incubated with $FeSO_4$ did not cause a detectable change in the ^{1}H-NMR spectrum, even after ~40 minutes of incubation (**figure 5C**), suggesting that SecA-MBD binds preferentially to iron.

Role of conserved serine in metal preference. The SecA MBD contains a strongly conserved serine residue, Ser-890 (**figure 1A**) (6), which is also conserved in the MBDs of both YecA and YchJ (**supporting figure S4**). It is unlikely that Ser-890 is directly involved in the interaction of the MBD with SecB since it is not located on the SecB-interaction surface (10). Furthermore, Ser-890 is conserved in the N-terminal MBD of YchJ, which lacks the amino acid residues required for binding to SecB. However, SecA-MBD containing an alanine substitution at this position (SecA-MBD^{S890A}) exchanged iron for zinc at a detectable rate (**figure 5D**), suggesting that Ser-890 is important for the folding of the MBD and/or coordination of the metal.

Binding affinity of SecA-MBD peptides for Zn^{2+}. To determine whether the alanine substitution caused a general defect in metal binding, we determined the affinity of SecA-MBD and SecA-MBD^{S890A} for Zn^{2+} using isothermal titration calorimetry (ITC). The affinity of the wild-type SecA-MBD for Zn^{2+} (36.0 ± 11.6 nM; **supporting figure S5A**) was not significantly different from that of SecA-MBD^{S890A} (46.0 ± 9.0 nM; **supporting figure S5B**), suggesting that the substitution does not affect its affinity for Zn^{2+}. We could not determine the affinity for SecA-MBD for iron due to the interfering heat exchange caused by aerobic oxidation of Fe^{2+} and because binding of SecA-MBD to Fe^{3+} did not cause a detectable heat exchange. Nonetheless, these results, taken together with the ^{1}H-NMR experiments, suggested that the serine-to-alanine substitution specifically affects the affinity of SecA-MBD^{S890A} for iron.

DISCUSSION

Our results indicate that iron is a physiological ligand of SecA-like MBDs. Analysis of the metal content of purified YecA and YchJ by mass spectrometry and absorbance spectroscopy indicate that both proteins copurify with significant amounts of iron. Indeed, SecA itself copurified with iron. EPR experiments indicated that both YecA and the SecA-MBD peptide bind to iron, and structural analysis of YecA by NMR indicates that it binds to iron via its C-terminal MBD. Finally, ^{1}H-NMR and ITC experiments suggest that the SecA MBD displays a binding preference for iron and that this specificity is determined in part by a conserved serine.

Previous studies suggested that zinc is the physiological ligand of the SecA MBD because it co-purifies with Zn^{2+} (7). However, many iron-binding proteins have a high intrinsic affinity for zinc (14), and unlike iron, zinc is stable under aerobic conditions. Purification of SecA typically takes several hours, and without extraordinary effort, zinc typically contaminates water, salts and glassware used to make purification buffers in significant amounts (15). For example, ICP-MS analysis suggested that our purification buffers typically contained ~300 nM zinc. It is therefore possible that iron is displaced by zinc during

purification. Other factors, such as the presence of reducing agents and overproduction of the protein, could exacerbate this issue.

The strong conservation of Ser-890 in SecA-like MBDs suggests that these MBDs normally also bind to iron *in vivo*. Although Ser-890 is not involved in coordinating the Zn^{2+} ion in structures of the MBD (6,10), its hydroxyl group points inward toward the metal-binding site. These structures also suggest that the tetrahedral coordination of zinc by Cys-886, -888 and -897 and His-898 is strained (6). It is possible that octahedral coordination of iron by these residues and Ser-890 could relieve this strain (16). Indeed, copper, which can be coordinated octahedrally, copurifies in significant amounts with YecA and YchJ and stabilises binding to SecB to a greater extent than Zn^{2+} (7,14). However, it is unlikely that copper is a physiological ligand since it is not normally found in the cytoplasm (14).

Finally, the affinity of the SecA MBD peptide for Zn^{2+} suggests that zinc is not a physiological ligand. ITC indicated that SecA-MBD binds to Zn^{2+} with a K_D of ~40 nM, and competition experiments suggested that it binds to iron with a similar or higher affinity. These affinities are consistent with cytoplasmic iron-binding proteins and the cytoplasmic concentration of iron (50-100 nM) but not that of zinc (pM) (14,16,17).

EXPERIMENTAL PROCEDURES

Chemicals and media. All chemicals were purchased from Fisher or Sigma-Aldrich unless indicated. Synthetic peptides were synthesised by Severn Biotech (Kidderminster, UK) or using an in-house synthesiser. The quality of the peptides was checked using MALDI mass spectrometry. 100X EDTA-free protease inhibitor cocktail was purchased from Pierce (Thermo-Fisher). Cells were grown using LB medium (18). Where indicated, IPTG was added to the culture medium. Where required, kanamycin (30 μg/ml) was added to the growth medium.

Purification of YecA and YchJ. The *yecA* and *ychJ* genes from *Escherichia coli* K-12 were fused in-frame to the 3′ end of the gene encoding SUMO from *S. cerevisiae* in plasmid pCA528 and purified as described previously (19). A detailed description of the purification of YecA and YchJ, can be found in the supporting information.

Metal ion analysis. The metal ion content of purified YecA and YchJ was determined using ICP-MS (School of GEES, University of Birmingham). The 5 kDa MWCO concentrator filtrate (Sartorius, Göttingen, Germany) was used to control for the amount of unbound metal in the protein samples. The zinc and iron ion content of the EDTA eluate from the Ni-NTA column after purification in the presence of 1 mM TCEP was determined using ICP-OES (School of GEES).

Absorbance spectroscopy. The absorbance spectra of 200 μl of 600-800 μM purified YecA or YchJ in buffer 1 (20 mM potassium HEPES, pH 7.5, 100 mM potassium acetate, 10 mM magnesium acetate) were determined from 300-600 nm using a CLARIOstar plate reader (BMG Labtech) using UV-clear flat bottomed 96-well plates (Greiner). The absorbance spectrum for the buffer alone was subtracted from that of the purified protein, and the absorbance was normalised to the concentration of the protein in the sample.

EPR spectroscopy. EPR samples were suspended in 50 μl buffer containing 30% glycerol. For YecA, samples contained 0.85 mM $FeCl_3$ or 0.6 mM YecA and $FeCl_3$. For SecA-MBD, samples contained 0.5 mM $FeSO_4$, which had been left to oxidize aerobically, alone or with 0.5 mM SecA-MBD. The EPR spectra of the samples was determined as described in the supporting information. The resultant echo-detected field swept profiles were normalised for plotting, taking account of differences in video gain, concentration and numbers of averages.

NMR backbone assignment of YecA. The ^{1}H, ^{15}N, and ^{13}C resonances of the YecA backbone were assigned using BEST TROSY versions of HNCA, HN(CO)CA, HNCACB, HN(CO)CACB, HNCO and HN(CA)CO (20-26). All spectra were acquired using a Bruker 900 MHz spectrometer equipped with a 4-channel AVANCE III HD console and a 5mm TCI z-PFG cryogenic probe. A detailed description of the experimental conditions can be found in the supporting information. Non-uniformed sampled data were reconstructed using the compressed sensing algorithm with MDDNMR (27) and processed using nmrPipe (28). Spectra were analysed in Sparky (29).

Determination of metal content of SecA-biotin. 100 ml cultures of DRH839 (MC4100 ΔsecA λ-p_{trc}-*secA-biotin*..SpecR) (13) were grown

in 10 μM or 100 μM IPTG to OD_{600} ~ 1. Cells were lysed using cell disruption, and lysates were incubated with 100 μl Streptactin-sepharose (IBA Lifesciences, Göttingen, Germany) for 15 minutes. The beads were washed four times with 30 ml buffer (50 mM potassium HEPES, pH 7.5, 100 mM potassium acetate, 10 mM magnesium acetate, 0.1% nonidet P40). Metal was eluted from the beads by incubating with 10 mM HEPES, pH 7.5, 50 mM EDTA) at 55˚C for 30 minutes, and the zinc and iron content was determined using ICP-OES. The amount of bound protein was determined by boiling in SDS sample buffer and analysing using Bradford reagent (BioRad, Hercules, CA). The eluted protein was resolved on a BioRad 15% TGX gel.

^{1}H-NMR of SecA-MBD. All spectra were obtained at 298 K on a Bruker 900 MHz spectrometer equipped with a cryogenically cooled 5mm TCI probe using excitation sculpting for water suppression on a sample in 90% H_2O/10% D_2O. Sequence specific assignments were completed using a TOCSY experiment in 90% H_2O/10% D_2O using a DIPSI2 spin-lock with a mixing time of 65 ms, 32 transients and collecting 512 increments with a spectral width of 10 ppm in both dimensions. 1D data sets comprised 16 transients, 32000 data points and a spectral width of 16 ppm. All data were processed using Topspin 3.2.6 software using an exponential window function with a line broadening of 1 Hz.

ITC. ITC measurements were carried out in a MicroCal VP-ITC calorimeter (Piscataway, NJ, USA). All solutions were centrifuged for 5 min at 13,000 rpm and then thoroughly degassed under vacuum for 5 min with gentle stirring immediately before use. 0.1mM $ZnSO_4$ was titrated into a solution of the indicated peptide (0.01 mM) in the sample cell (Vo = 1.4037 ml). Titrations consisted of a preliminary 2 μl injection followed by 50 6 μl injections of 12 s duration with 700 s between each injection. All experiments were carried out at 25˚C with an initial reference power of 10 μcal/s. The raw data were analysed with Origin 7.0 using one-binding site model and were corrected for the heat of dilution of the metal ion in the absence of peptide.

ABBREVIATIONS

BEST, band-selective short transient excitation; DIPSI, decoupling in the presence of scalar interactions; DTT, dithiothreitol; EDTA, ethylene diamine tetra-acetic acid; EPR, electron paramagnetic resonance; HSQC, heteronuclear single quantum coherence; ICP, inductively coupled plasma; IPTG, isopropyl-β-thiogalactoside; ITC, isothermal titration calorimetry; MS, mass spectrometry; NMR, nuclear magnetic resonance; NTA, nitrilotriacetic acid; OES, optical emission spectrometry; SUMO, small ubiquitin-like modifier; TCEP, tris(2-carboxyethyl)phosphine; TOCSY, total correlated spectroscopy; TROSY, transverse relaxation optimised spectroscopy; UPF, unidentified protein function; UV, ultraviolet

ACKNOWLEDGEMENTS

We thank J. Cole, J. Green, A. Peacock and O. Daubney for advice and assistance. We thank Drs S. Baker, M. Thompson, H. El Mkami and A. Shah for technical assistance and members of the Henderson, Lund and Grainger labs for insightful discussions. TCS was funded by the Biotechnology and Biological Sciences Research Council (BBSRC) Midlands Integrated Integrative Biosciences Training Partnership (MIBTP). MA was funded by Jouf University. DH and MJ were funded by BBSRC grant BB/L019434/1. TK was funded by BBSRC grant BB/P009840/1. J.E.L. thanks the Royal Society for a University Research Fellowship and the Wellcome Trust for the Q-band EPR spectrometer (099149/Z/12/Z). NMR work was supported by the Wellcome Trust (099185/Z/12/Z), and we thank HWB-NMR at the University of Birmingham for providing open access to their Wellcome Trust-funded 900 MHz spectrometer.

CONFLICTS OF INTEREST

The authors declare that they have no conflicts of interest with the contents of this article.

REFERENCES

1. Beckwith, J. (2013) The Sec-dependent pathway. *Research in microbiology* **164**, 497-504

2. Tsirigotaki, A., De Geyter, J., Sostaric, N., Economou, A., and Karamanou, S. (2017) Protein export through the bacterial Sec pathway. *Nat Rev Microbiol* **15**, 21-36
3. Park, E., and Rapoport, T. A. (2012) Mechanisms of Sec61/SecY-mediated protein translocation across membranes. *Annu Rev Biophys* **41**, 21-40
4. Cranford Smith, T., and Huber, D. (2018) The way is the goal: how SecA transports proteins across the cytoplasmic membrane in bacteria. *FEMS Microbiol Lett* **365**
5. Collinson, I., Corey, R. A., and Allen, W. J. (2015) Channel crossing: how are proteins shipped across the bacterial plasma membrane? *Philos Trans R Soc Lond B Biol Sci* **370**
6. Dempsey, B. R., Wrona, M., Moulin, J. M., Gloor, G. B., Jalilehvand, F., Lajoie, G., Shaw, G. S., and Shilton, B. H. (2004) Solution NMR structure and X-ray absorption analysis of the C-terminal zinc-binding domain of the SecA ATPase. *Biochemistry* **43**, 9361-9371
7. Fekkes, P., de Wit, J. G., Boorsma, A., Friesen, R. H., and Driessen, A. J. (1999) Zinc stabilizes the SecB binding site of SecA. *Biochemistry* **38**, 5111-5116
8. Fekkes, P., van der Does, C., and Driessen, A. J. (1997) The molecular chaperone SecB is released from the carboxy-terminus of SecA during initiation of precursor protein translocation. *Embo J* **16**, 6105-6113
9. Randall, L. L., and Hardy, S. J. (2002) SecB, one small chaperone in the complex milieu of the cell. *Cell Mol Life Sci* **59**, 1617-1623
10. Zhou, J., and Xu, Z. (2003) Structural determinants of SecB recognition by SecA in bacterial protein translocation. *Nat Struct Biol* **10**, 942-947
11. The UniProt, C. (2017) UniProt: the universal protein knowledgebase. *Nucleic Acids Res* **45**, D158-D169
12. Finn, R. D., Bateman, A., Clements, J., Coggill, P., Eberhardt, R. Y., Eddy, S. R., Heger, A., Hetherington, K., Holm, L., Mistry, J., Sonnhammer, E. L., Tate, J., and Punta, M. (2014) Pfam: the protein families database. *Nucleic Acids Res* **42**, D222-230
13. Huber, D., Jamshad, M., Hanmer, R., Schibich, D., Doring, K., Marcomini, I., Kramer, G., and Bukau, B. (2017) SecA Cotranslationally Interacts with Nascent Substrate Proteins In Vivo. *J Bacteriol* **199**
14. Waldron, K. J., and Robinson, N. J. (2009) How do bacterial cells ensure that metalloproteins get the correct metal? *Nat Rev Microbiol* **7**, 25-35
15. Graham, A. I., Hunt, S., Stokes, S. L., Bramall, N., Bunch, J., Cox, A. G., McLeod, C. W., and Poole, R. K. (2009) Severe zinc depletion of Escherichia coli: roles for high affinity zinc binding by ZinT, zinc transport and zinc-independent proteins. *J Biol Chem* **284**, 18377-18389
16. Waldron, K. J., Rutherford, J. C., Ford, D., and Robinson, N. J. (2009) Metalloproteins and metal sensing. *Nature* **460**, 823-830
17. Osman, D., Martini, M. A., Foster, A. W., Chen, J., Scott, A. J. P., Morton, R. J., Steed, J. W., Lurie-Luke, E., Huggins, T. G., Lawrence, A. D., Deery, E., Warren, M. J., Chivers, P. T., and Robinson, N. J. (2019) Bacterial sensors define intracellular free energies for correct enzyme metalation. *Nature Chemical Biology*
18. Miller, J. H. (1992) *A Short Course in Bacterial Genetics*, Cold Spring Harbor Press, Cold Spring Harbor, NY
19. Andreasson, C., Fiaux, J., Rampelt, H., Mayer, M. P., and Bukau, B. (2008) Hsp110 is a nucleotide-activated exchange factor for Hsp70. *J Biol Chem* **283**, 8877-8884
20. Clubb, R. T., Thanabal, V., and Wagner, G. (1992) A Constant-Time 3-Dimensional Triple-Resonance Pulse Scheme to Correlate Intraresidue H-1(N), N-15, and C-13(') Chemical-Shifts in N-15-C-13-Labeled Proteins. *Journal of magnetic resonance* **97**, 213-217
21. Grzesiek, S., and Bax, A. (1992) Improved 3d Triple-Resonance Nmr Techniques Applied to a 31-Kda Protein. *Journal of magnetic resonance* **96**, 432-440
22. Lescop, E., Schanda, P., and Brutscher, B. (2007) A set of BEST triple-resonance experiments for time-optimized protein resonance assignment. *Journal of magnetic resonance* **187**, 163-169

23. Kay, L. E., Keifer, P., and Saarinen, T. (1992) Pure Absorption Gradient Enhanced Heteronuclear Single Quantum Correlation Spectroscopy with Improved Sensitivity. *Journal of the American Chemical Society* **114**, 10663-10665
24. Salzmann, M., Wider, G., Pervushin, K., Senn, H., and Wuthrich, K. (1999) TROSY-type triple-resonance experiments for sequential NMR assignments of large proteins. *Journal of the American Chemical Society* **121**, 844-848
25. Schanda, P., Van Melckebeke, H., and Brutscher, B. (2006) Speeding up three-dimensional protein NMR experiments to a few minutes. *Journal of the American Chemical Society* **128**, 9042-9043
26. Salzmann, M., Pervushin, K., Wider, G., Senn, H., and Wuthrich, K. (1998) TROSY in triple-resonance experiments: New perspectives for sequential NMR assignment of large proteins. *P Natl Acad Sci USA* **95**, 13585-13590
27. Kazimierczuk, K., and Orekhov, V. Y. (2011) Accelerated NMR spectroscopy by using compressed sensing. *Angew Chem Int Ed Engl* **50**, 5556-5559
28. Delaglio, F., Grzesiek, S., Vuister, G. W., Zhu, G., Pfeifer, J., and Bax, A. (1995) NMRPipe: a multidimensional spectral processing system based on UNIX pipes. *J Biomol NMR* **6**, 277-293
29. Lee, W., Tonelli, M., and Markley, J. L. (2015) NMRFAM-SPARKY: enhanced software for biomolecular NMR spectroscopy. *Bioinformatics* **31**, 1325-1327

FIGURE LEGENDS

Figure 1

A

```
E. coli              GERKVGRNDPCPCGSGKKYKQCHGRLQ
R. loti              TWGKVGRNEACPCGSGKKYKHCHGAFA
B. subtilis          KVVDIGRNAPCHCGSGKKYKNCCGRTE
L. lactis            SFENVGRNDLCPCGSGKKFKNCHGRTHIA
T. pallidum          AGAKVGRNTPCPCGSGKKYKHCCGR
B. longum            TFPGTGKNAPCPCGSGRKYKMCHGQNEA
B. thetaiotamicron   AEKTVGRNDPCPCGSGKKYKNCHGQNA
YecA                 AEEKPGRNDPCPCGSGKKFKQCCLH
YchJ N-term                MSQLCPCGSAVEYSLCCHPY…
YchJ C-term          TRPQFGRNDPCPCGSGKKFKKCCGQ
MBD-SecA^S890A       GERKVGRNDPCPCGAGKKYKQCHGRLQ
```

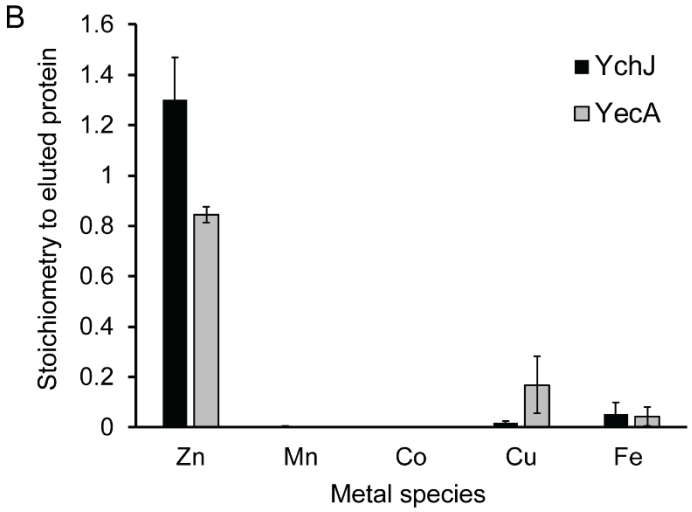

Figure 1. Copurification of metals with YecA and YchJ. (A) Sequence alignment of the MBDs of SecA from *Escherichia coli*, *Rhizobium loti*, *Bacillus subtilis*, *Lactococcus lactis*, *Treponema pallidum*, *Bifidobacterium longum* and *Bacteriodes thetaiotamicron*, YecA from *Escherichia coli*, the N- and C-terminal MBDs of YchJ from *Escherichia coli* and the MBD-SecA^{S890A} peptide. The conserved metal-coordinating amino acids at positions 886, 888, 897 and 898 in *E. coli* SecA are bolded in black and starred. The conserved serine residue at position 890 in *E. coli* SecA is bolded in red. (B) His-SUMO-YecA and His-SUMO-YchJ were purified using Ni-affinity chromatography, and the amount of co-purifying Zn, Mn, Co, Cu and Fe were determined by ICP-MS. The concentrations of the extracted metals were normalised to the amount of purified protein. Confidence intervals are one standard deviation.

Figure 2

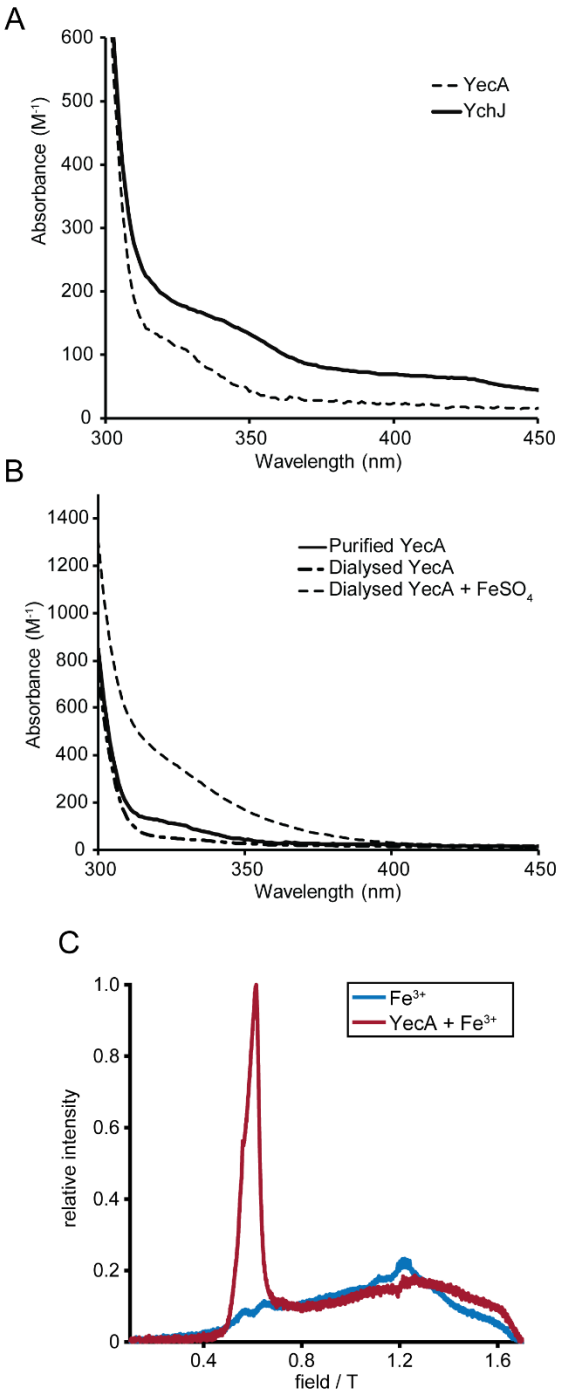

Figure 2. Spectroscopic analysis of iron binding by YecA and YchJ. (A) Buffer subtracted absorbance spectra YecA (dashed) and YchJ (solid black). The absorbance at each wavelength was normalised to the concentration of the MBD(s) (*i.e.* to the concentration of YecA and twice the concentration of YchJ). (B) Buffer subtracted absorbance spectra of purified YecA (solid black), purified YecA that was dialysed against EDTA (dash-dot) and EDTA-dialysed YecA to which an equimolar concentration of $FeSO_4$ was added (dashed). The absorbance spectra were normalised to the concentration of YecA. (C) The echo-detected field swept EPR spectrum of $FeCl_3$ was determined in the absence (blue trace) or presence (red trace) of YecA.

Figure 3

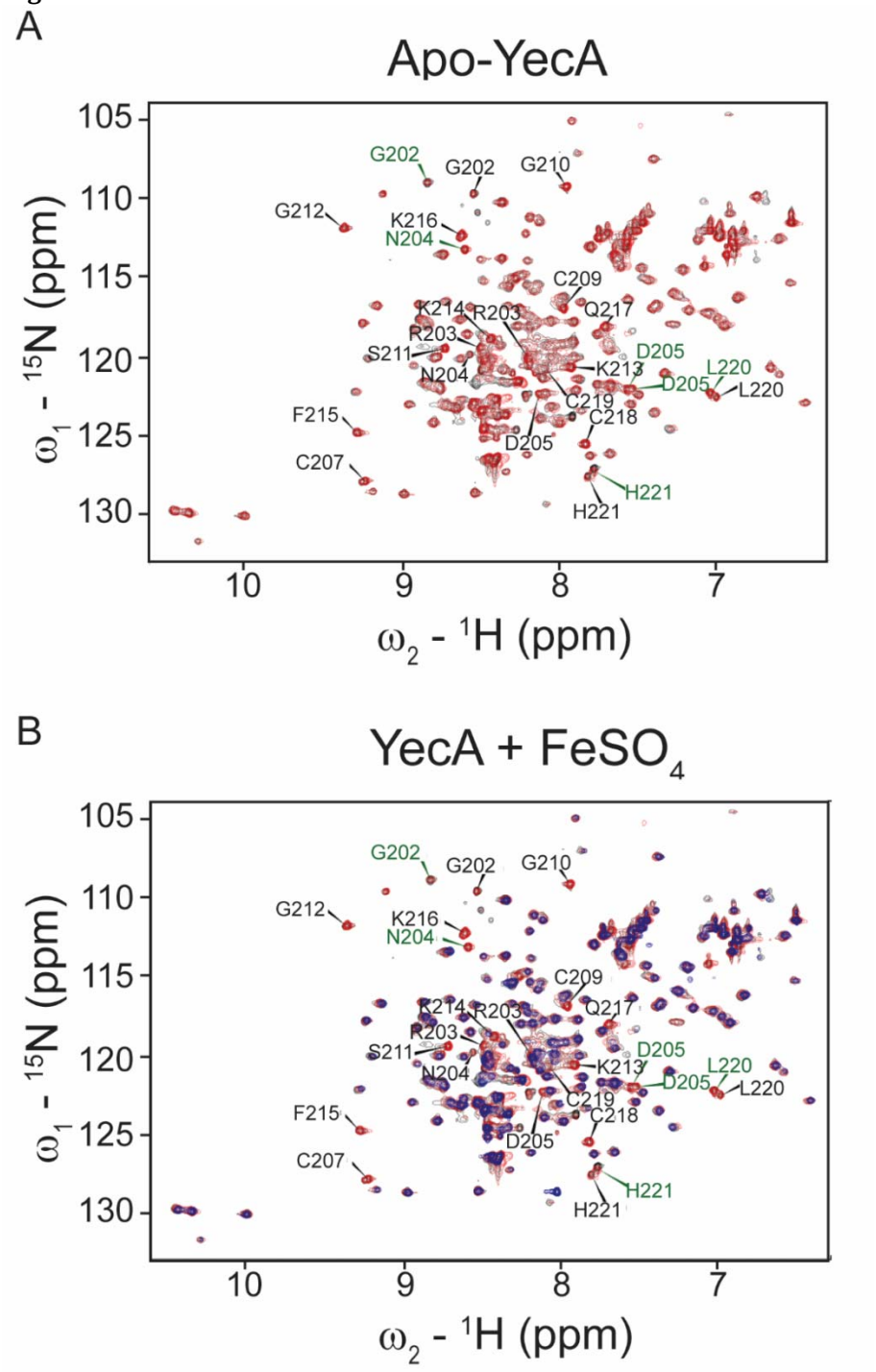

Figure 3. YecA binds to iron *via* its MBD. (A) TROSY spectrum of metal-free ^{15}N & ^{13}C-labelled YecA. The ^{1}H, ^{15}N, and ^{13}C resonances of the polypeptide backbone for the C-terminal 20 amino acids (excluding prolines-206 and -208) were assigned using triple resonance experiments. Resonances of amino acids in the MBD are indicated with arrowheads. Amino acids producing two resonance peaks are labelled in green. (B) Overlay of the TROSY spectra of metal-free YecA (red) and YecA in the presence of equimolar concentrations of $FeSO_4$ (blue). The absence of a blue peak suggests that the amino acid producing the resonance is in the proximity of the bound iron.

Figure 4

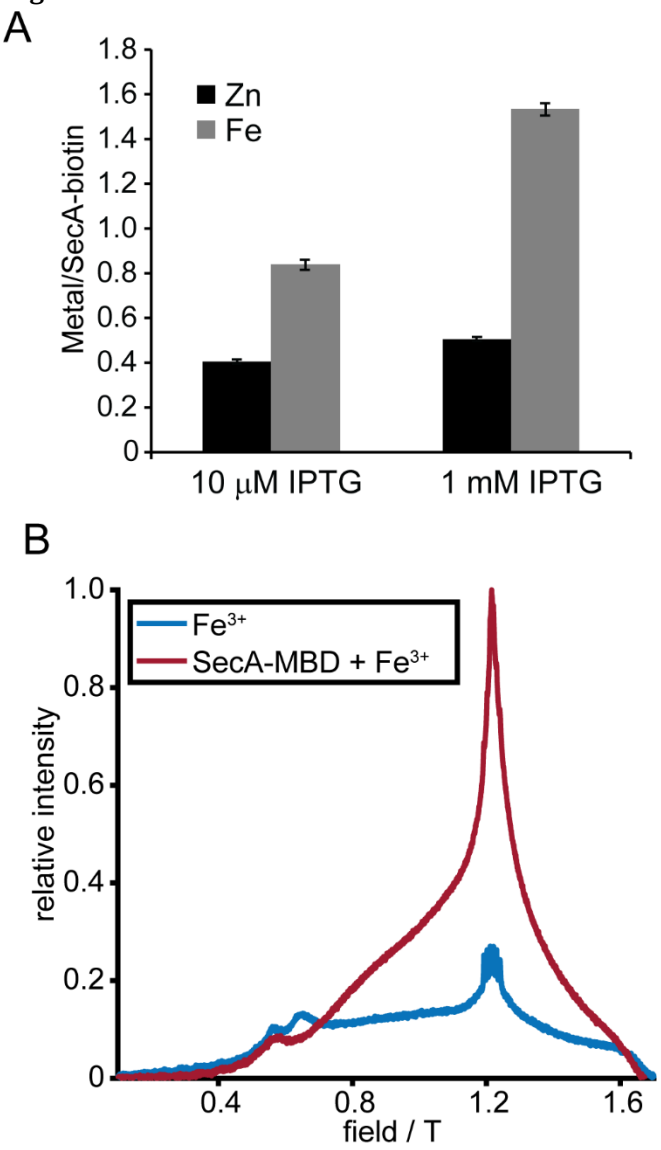

Figure 4. The SecA MBD binds to iron *in vivo* and *in vitro*. (A) DRH839 cells (Δ*secA* p_{trc}-*secA-biotin*) were grown in the presence of 10 μM or 1 mM IPTG to induce expression of SecA-biotin. Cells were rapidly lysed by cell disruption, incubated with streptavidin-sepharose and washed extensively with buffer. The zinc and iron content of the EDTA eluate was determined using ICP-OES and normalised to the amount of protein bound to the streptavidin beads (B) The echo-detected field swept EPR spectrum of oxidised $FeSO_4$ was determined in the absence (blue trace) or presence (red trace) of SecA-MBD.

Figure 5

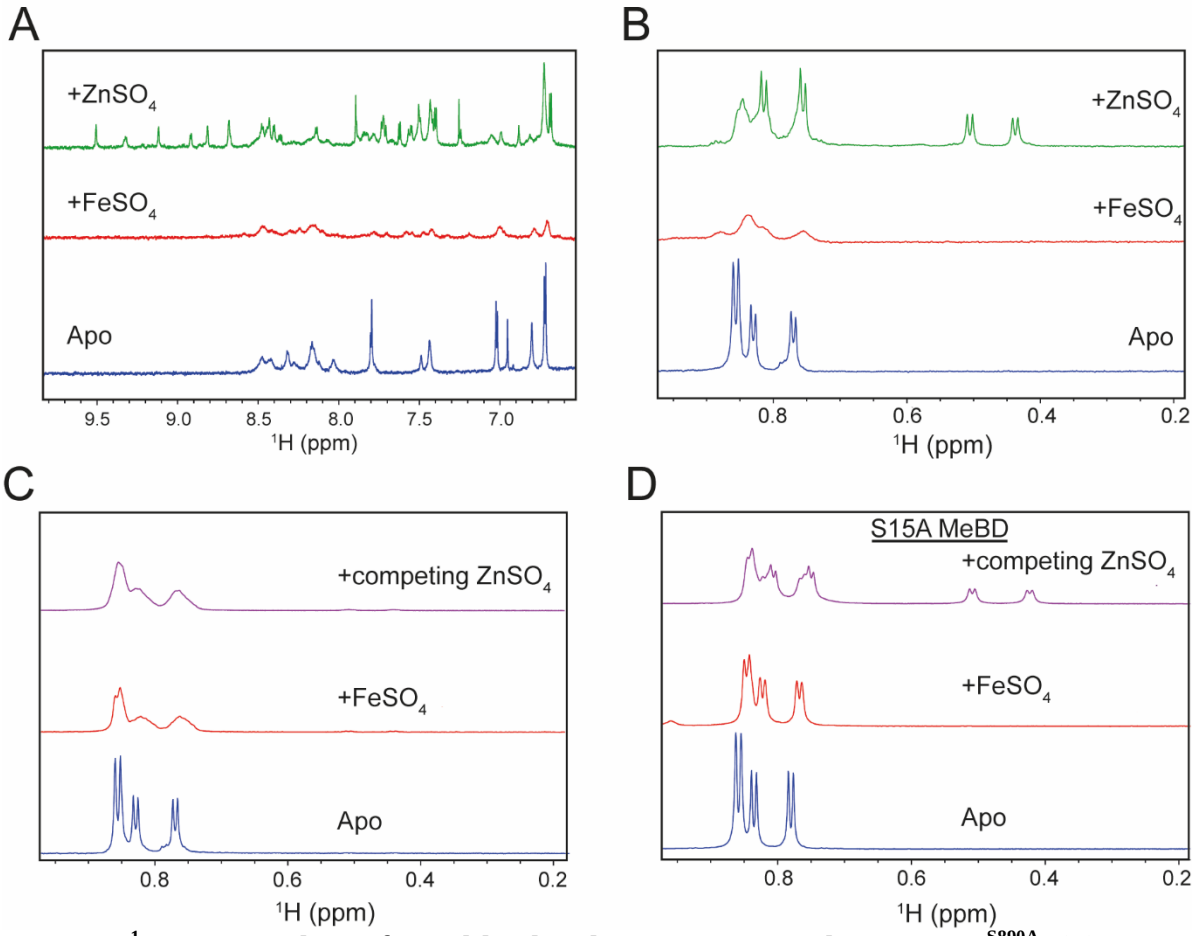

Figure 5. ^{1}H-NMR analysis of metal binding by SecA-MBD and SecA-MBD^{S890A}. (A) 6.5-10 ppm region of the ^{1}H-NMR spectra of SecA-MBD in the absence (blue) or presence of equimolar concentrations of $FeSO_4$ (red) or $ZnSO_4$ (green). The appearance of resonances in the ~8.5-10 ppm region in the presence of $ZnSO_4$ indicates the formation of secondary structure. The strong quenching of the resonances in the presence of $FeSO_4$ is due to proximity to the bound iron ion. (B) 0.2-1.0 ppm region of the ^{1}H-NMR spectra of SecA-MBD in the absence (blue) or presence of equimolar concentrations of $FeSO_4$ (red) or $ZnSO_4$ (green). Binding of SecA-MBD to zinc results in a shift of the resonances corresponding to the methyl ^{1}Hs of valine, and binding of SecA-MBD to iron results in a significant broadening and flattening of these resonances. (C & D) 0.2-1.0 ppm region of the ^{1}H-NMR spectra of SecA-MBD (C) or SecA-MBD^{S890A} (D) in the absence of metal (blue), in the presence of equimolar $FeSO_4$ (red) and after the addition of competing concentrations of $ZnSO_4$ to the iron-bound peptide after >10 minutes of equilibration at room temperature (purple).

Supporting figure S1.

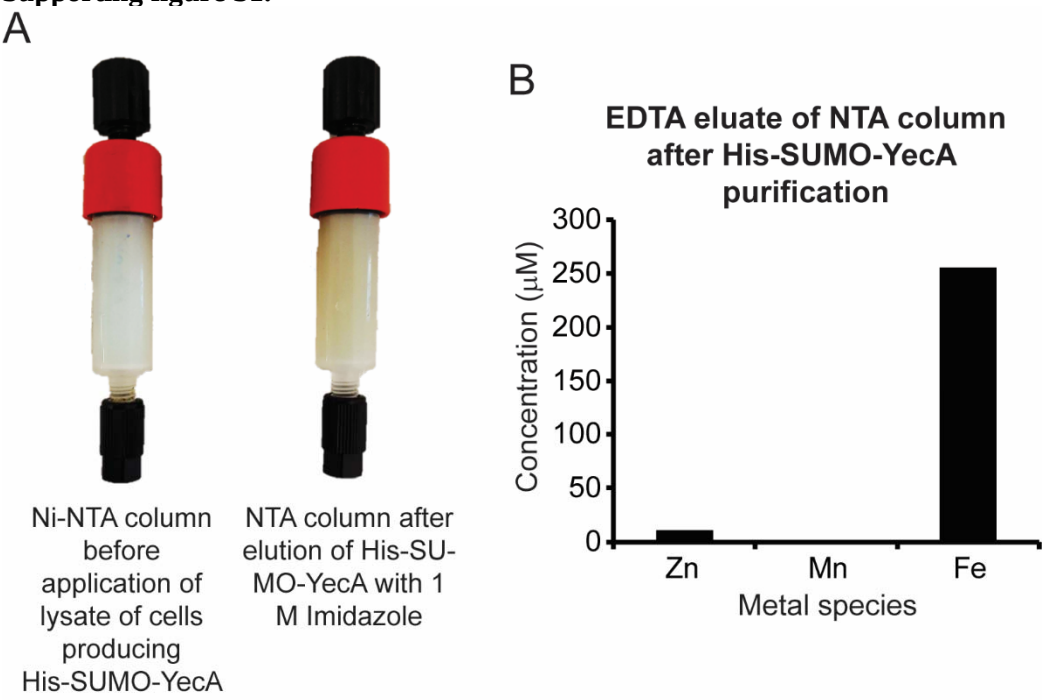

Supporting figure S1. Analysis of the EDTA eluate from columns used to purify YecA. Lysates of BL21(DE3) producing His-SUMO-YecA were passed over a Ni-NTA column and washed extensively with buffer containing 50 mM imidazole and 1 mM TCEP. (A) Pictures of a 1 ml Ni-NTA before applying cell lysate (left) and after elution of the bound protein using buffer containing 1 M imidazole (right). (B) The residual metal bound by the Ni-NTA column after elution of the bound protein was stripped from the column using 1 mM EDTA, and the zinc, manganese and iron content of the EDTA eluate was determine using ICP-OES.

Supporting figure S2.

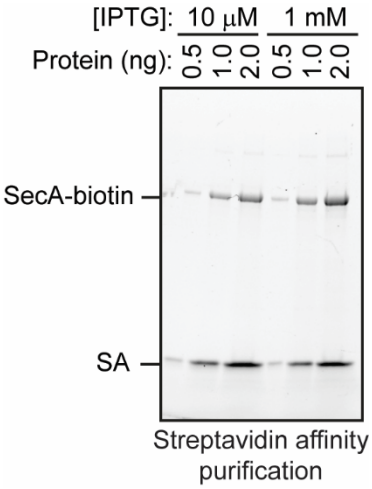

Supporting figure S2. Analysis of purified SecA-biotin. DRH839 cells (Δ*secA* p_{trc}-*secA-biotin*) were grown in the presence of 10 μM or 1 mM IPTG, and SecA-biotin was purified from the cells using streptavidin-coated sepharose beads. After elution of the bound metal protein as described in figure 6, the protein was eluted from the beads by boiling in 1X Laemmli buffer, and the protein concentration in the samples was determined using Bradford. The indicated amount of protein was loaded on SDS-PAGE gel and visualised using Bio-Rad Stain-free technology. SA; streptavidin.

Supporting figure S3.

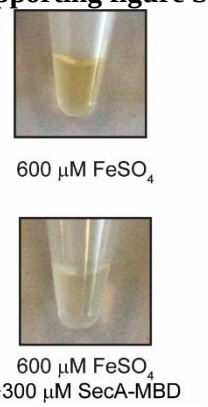

Supporting figure S3. SecA-MBD peptide protects $FeSO_4$ from formation of iron oxides. 600 μM $FeSO_4$ was incubated in the absence (above) or presence (below) of a 300 μM solution of a synthetic peptide consisting of the C-terminal 27 amino acids of SecA (SecA-MBD) and incubated at room temperature for 15 minutes.

Supporting figure S4

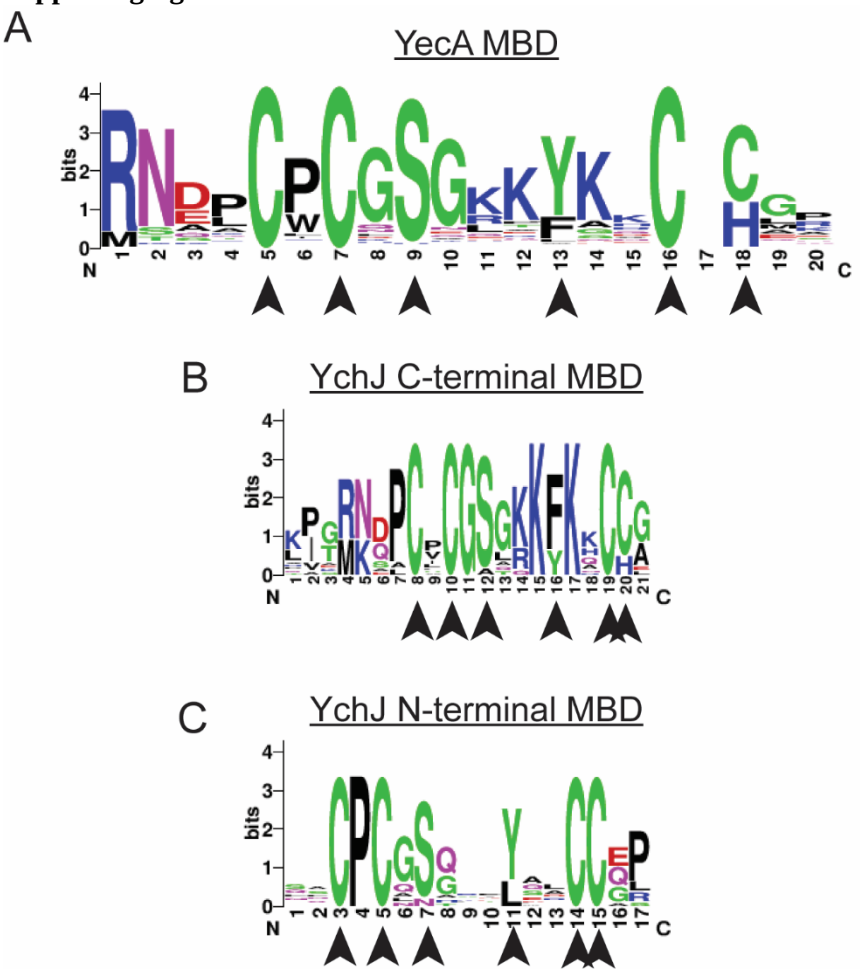

Supporting figure S4. Consensus sequences of the YecA and YchJ MBDs. Logos representing the consensus sequences of the YecA MBD (A), the C-terminal YchJ MBD (B) and the N-terminal YchJ MBD (C) were constructed from the alignments of 10 sequences for YecA, 16 sequences for the YchJ C-terminal MBD and 15 sequences for the YchJ N-terminal MBD from NCBI.

Supporting figure S5

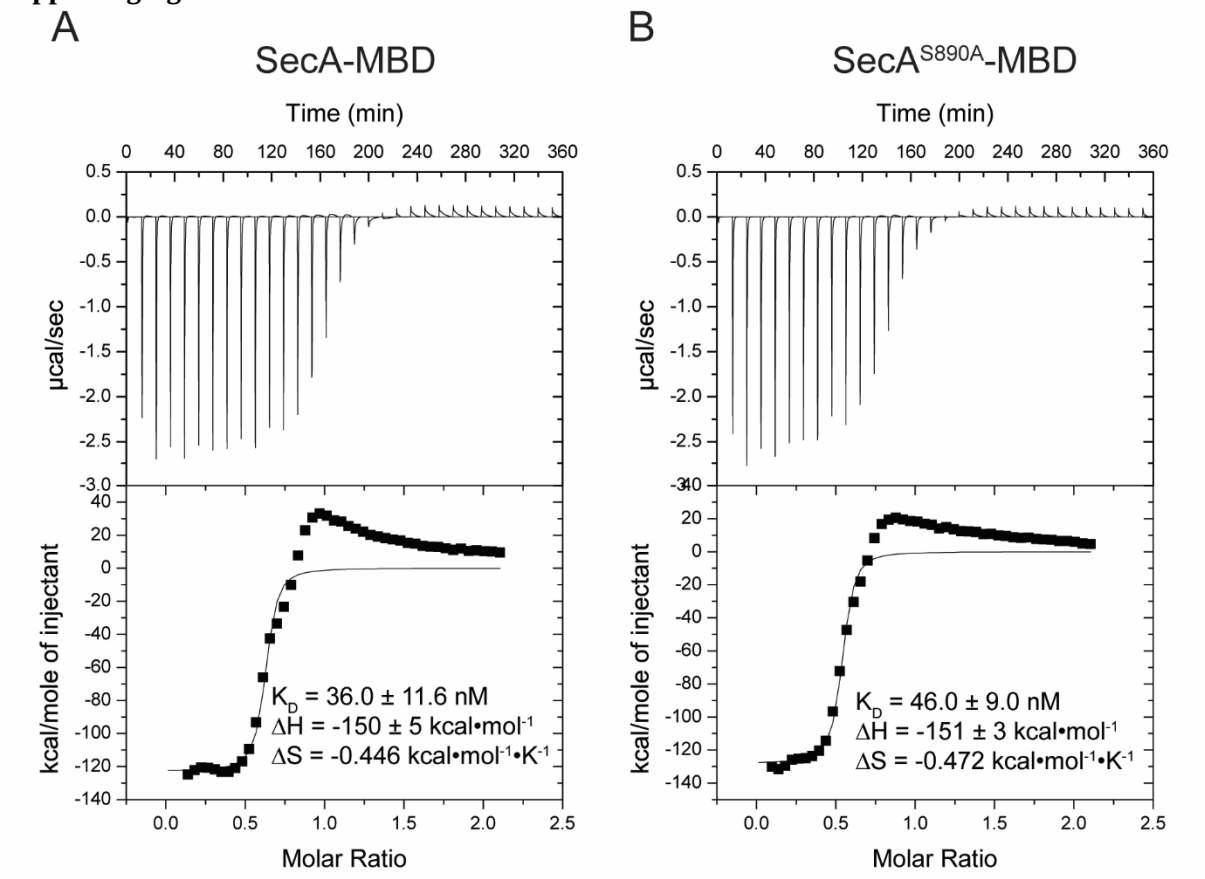

Supporting figure S5. Determination of the affinity of SecA-MBD and SecA-MBD^{S890A} for Zn^{2+} by ITC. The heat exchange upon mixing solutions containing SecA-MBD peptide (A) and SecA-MBD^{S890A} peptide (B) with $ZnSO_4$ was measured by isothermal titration calorimetry (ITC; above). K_D, ΔH and ΔS determined from fits of the heat exchange curves (below).

SUPPLEMENTAL METHODS

Purification of YecA and YchJ. For identification of the copurifying metals and absorbance spectroscopy, BL21(DE3) cells containing the SUMO-YecA and SUMO-YchJ plasmids were grown to OD_{600} 1.0 at 37°C. Cells were then shifted to 25°C and grown overnight in the presence of 1 mM IPTG. Cells were lysed in buffer 1 (20 mM potassium HEPES, pH 7.5, 100 mM potassium acetate 10 mM magnesium acetate) containing protease inhibitor by cell disruption. Where indicated, TCEP was added at a concentration of 1 mM. Lysates were passed over a 1 ml His-Trap HF column (GE Healthcare). The bound protein was washed with 15 ml buffer 1 containing 500 mM potassium acetate and 50 mM imidazole) and 15 ml buffer 1 containing 50 mM imidazole and was eluted using buffer 1 containing 500 mM imidazole. The eluted protein was dialysed against buffer 1 to remove the imidazole and concentrated using concentrators with a 5 kDa cutoff (Vivaspin).

For HSQC-NMR analysis of YecA, cells containing the YecA plasmid were grown in M9 minimal media containing $^{15}NH_4Cl$, $^{1}H_7$-$^{13}C_6$-glucose (2 g/l) and trace minerals. Cultures were grown to OD_{600} 0.8 at 37°C, shifted to 18°C and induced overnight with 1mM IPTG. Cells were lysed by cell disruption and purified using a 1 ml His-Trap column as described above. After elution, the protein was treated with purified hexahistine-tagged Ulp1 from *S. cerevisiae* to remove the SUMO tag and dialysed overnight against buffer 1 containing 5 mM β-mercaptoethanol to remove the imidazole. The SUMO tag and Ulp1 protease were removed from the purified protein by passing the cut protein over a 1 ml His-Trap column. Purified YecA was then concentrated using anion exchange chromatography, and the eluate was dialyzed against buffer 1 containing 5 mM β-mercaptoethanol and 1 mM EDTA.

NMR backbone assignment of YecA. Assignment spectra were acquired on 0.5 mM ^{15}N, ^{13}C-labelled protein in 20 mM [MES]-NaOH [pH 6.0], 10 mM NaCl, 10% D_2O in a 5 mm Shigemi tube (Shigemi Inc.). The ^{1}H, ^{15}N, and ^{13}C resonances of the YecA backbone were assigned using BEST TROSY versions of HNCA, HN(CO)CA, HNCACB, HN(CO)CACB, HNCO and HN(CA)CO (20-26). All experiments were performed at 298 K and acquired with a spectral width of 14 ppm in ^{1}H , collecting 1024 real data points, and 30 ppm in ^{15}N, collecting 92 increments. The centre of the spectra was set to 4.698 ppm in the ^{1}H and 118 ppm in ^{15}N. All spectra were acquired collecting 128 increments in the ^{13}C dimension using a non-uniform sampling scheme. The HN(CO)CACB and HNCACB experiments were acquired using 64 scans per increment, a spectral width of 76 ppm in the ^{13}C direction with the centre around 43.665 ppm. The HNCA and the HN(CO)CA experiments were acquired using 32 scans per increment, a ^{13}C spectral width of 30 ppm with the centre of the spectra set to 55.9 ppm. The HN(CA)CO and HNCO experiments were acquired using 32 scans per increment, a ^{13}C spectral width of 16 ppm centred around 176.2 ppm.

EPR spectroscopy. Measurements were taken with a Bruker Elexsys E580 spectrometer with an ER 5106QT-2w cylindrical resonator operating at 34 GHz, i.e. Q-band. Quartz tubes with 3 mm O.D. were used. Experiments were carried out at 10 K using a cryogen free variable temperature cryostat (from Cryogenic Limited). Echo-detected field sweeps were carried out by sweeping from 0.1 to 1.7 T with 4000 points using a Hahn echo sequence where the π pulse length was 32 ns and the time between pulses was 400 ns. The power level was determined by observing the maximum echo and was around 0.38 mW which is indicative of a high-spin system. The shot repetition time was set at 100 μs with 50 shots per point which was sufficient for the iron, though caused some saturation of the Mn^{2+} contaminant peak.